A novel methodology to assimilate sub-path flows in bi-level OD matrix estimation process

Krishna N.S. Behara, Ashish Bhaskar, and Edward Chung

***Abstract*— Traditional bi-level origin-destination (OD) matrix estimation process adjusts the matrix (at the upper level) based on the deviation between the observed and simulated traffic counts. The problem is mathematically highly underdetermined, and the quality of the solution can be enhanced by restricting the upper level search space with information from other sources. Addressing this need, this paper presents a methodology that assimilates additional structural information of sub-path flows in the aforementioned upper level objective function. By assuming assignment and sub-path proportion matrices are locally constant, the proposed objective function is differentiable, and the optimization can be achieved using gradient-based approach. The sub-path flows can be estimated from advanced data sources such as Bluetooth MAC scanner. The proposed methodology is tested using simulation on a real network from Brisbane, Australia and results indicate its practical relevance for situations when the penetration rate of Bluetooth trajectories is generally low and unknown. The proposed method has a better ability to maintain structural consistency in the OD estimates as compared to the traditional traffic counts-based approach; and considerable improvements in the quality of OD estimates are achieved even at lower penetration rates of sub-path flows.**

***Index Terms*: OD matrix estimation; bi-level optimization, Bluetooth; sub-path flows; gradient descent; OD structure; Brisbane, market penetration rates**

I. Introduction

Origin - destination (OD) matrix is a tabular representation of travel demand (flows) from different origins to destinations on the transport network. Such matrices are vital inputs for different levels of transport modelling- ranging from traditional strategic planning of transport infrastructure to advanced real-time operations and control of the network.

Ground truth of OD flows for large scale road network can't be directly measured with limited observations. Traditionally, road network is equipped with loop detectors and OD estimation process is modelled as a bi-level optimization problem [1, 2] where (*see* Fig.1): a) at upper level the OD matrix ($\mathbf{x}$) is adjusted by minimising the gap between the observed ($\tilde{\mathbf{y}}$) and estimated ($\mathbf{y}$) traffic counts; and b) at lower level traffic counts are estimated (simulated) by assigning traffic on the network using the adjusted OD matrix.

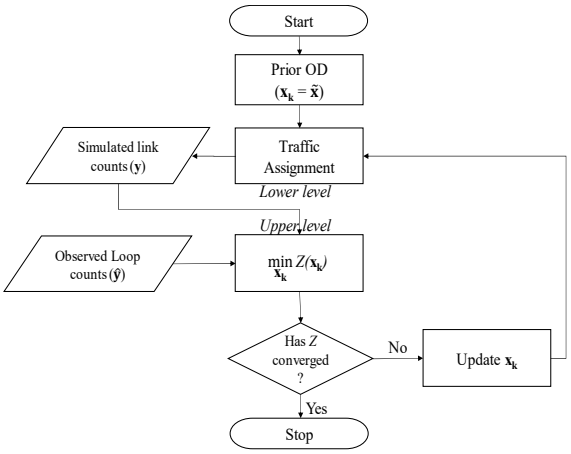

Fig. 1: Traffic counts-based bi-level OD estimation

In Fig.1, the upper level formulation, is generally expressed in terms of observed ($\tilde{\mathbf{y}}$) and estimated ($\mathbf{y}$) link flows and assumes one of the following forms: Information minimization/entropy maximization [3]; maximum likelihood approach [4]; Bayesian inference methods [5], and generalized least squares (GLS) [6]. The lower level of the bi-level framework runs traffic assignment ($\mathbf{P}$) that is either analytically derived [7] or simulation-based say, from Aimsun [8]. Equation 1 is the popular Spiess [9]'s formulation using matrix algebra where $^{\mathrm{T}}$ denotes the transpose operation.

$$\min_{\mathbf{x}} Z(\mathbf{x}) = \min_{\mathbf{x}} \frac{1}{2}\left(\left((\mathbf{y}-\tilde{\mathbf{y}})\right)^{\mathrm{T}}(\mathbf{y}-\tilde{\mathbf{y}})\right) \quad (1)$$

$$\text{subject to: } \mathbf{y} = \mathbf{P}\mathbf{x} \quad (1a)$$

Various techniques have been proposed to solve the above optimization function. This includes, fixed-point approaches [10], gradient-based [9], gradient approximations [11]; and evolutionary-algorithms (genetic algorithms, see [12]). Among these, gradient-based techniques are quite popular and different forms of the gradient based techniques are applied. This includes, coordinate descent method [13], mini-batch gradient descent [14], extended gradient method [15], projected gradient method [16], and the stochastic gradient method [17].

While most studies focused on developing new solution algorithms, estimating OD matrix using traffic counts is still an under-determined problem. This is because a number of combinations of OD flows (or OD matrices of different

Manuscript submitted for review on XX/XX/2019.

K.N.S. Behara is a Research Assistant and A. Bhaskar is Associate Professor in Queensland University of Technology, Brisbane, Australia (email: ashish.bhaskar@qut.edu.au).

E. Chung is a Professor in the Electrical Engineering Department, Hong Kong Polytechnic University, Hong Kong and is an Adjunct Professor at Queensland University of Technology.

structures) could exist to reproduce the same set of link flows, and thus the quality OD estimates cannot not be guaranteed if the objective function focusses only on the deviation of traffic counts [18]. This demands the need to maintain consistency in the structure of OD matrix (as per [19] the trip distribution pattern between different OD pairs within an OD matrix defines the OD structure) during every iteration of bi-level estimation process [20]. To preserve the OD structure, [21] proposed to use target trip matrix ($\tilde{\mathbf{x}}$) in the objective function in order to confine the feasible region of OD estimates (refer Equation 2); and many other studies [6, 16, 22-24] have later adopted this approach. The weight factors for objectives based on traffic counts and target OD matrix in Equation 2 are denoted by β_y and β_x, respectively.

$$\min_{\mathbf{x}} Z(\mathbf{x}) = \min_{\mathbf{x}} \frac{1}{2}\left(\left(\beta_y(\mathbf{y}-\tilde{\mathbf{y}})\right)^T(\mathbf{y}-\tilde{\mathbf{y}}) + \beta_x\left((\mathbf{x}-\tilde{\mathbf{x}})\right)^T(\mathbf{x}-\tilde{\mathbf{x}})\right) \quad (2)$$

$$\text{subject to: } \mathbf{y} = \mathbf{P}\mathbf{x} \quad (2a)$$

Researchers have also proposed constraints outside the objective function to maintain structural consistency. For instance, [20] proposed constraints on the columns of OD matrix using additional information from parking surveys, and [12] proposed constraints on the rows of OD matrix using the ratio of OD flows to origin flows. However, the prior knowledge (either in the form of target OD or trip production/attraction constraints) is based on outdated travel surveys and can lead to biased estimates [6].

With the availability of big traffic data, researchers have tried to address the OD under-determinacy problem by introducing vehicle trajectory information into the objective function formulation. [25-27] considered the deviations between the estimated and sub-path flows (from AVI measurements) by assuming that their market penetration rate is known. Few [28-30] developed methods to estimate the penetration rates. For instance, [28] used the deviations between estimated and observed link probe ratios (ratio of link flows observed from probes and loops) where the estimated link probe ratio is further dependent on OD probe ratio that is estimated using direct scaling method. [29] assumed that penetration rates of Bluetooth counts is same as that of Bluetooth trajectories, and used it to scale up the vehicle trajectories in the objective function. [30] used simulator-based approach to estimate the scaling factor of trajectories that are inferred from call detail records. Thus, no technique has been proposed until now to use the additional vehicle trajectories/sub-path flows information into the OD estimation formulation without prior knowledge of the penetration rates.

The sub-path in this paper is defined as the portion of vehicle's path inferred by series of sensors detections during the course of its complete traverse, and the observations of flows passing through the sub-path is referred as sub-path flows ($\tilde{\mathbf{s}}$). A sub-path can also be considered as a sequence of links. If it constitutes only two detections at the extreme ends of a road segment, then sub-path flows refer to link flows. If the vehicle's trip is continuously monitored (as in GPS) from its origin until its destination then sub-path represents a complete path. However, misdetections at a few sensor locations (as in case with Bluetooth scanners) could result in many such sub-paths for the same vehicle. In such cases the trips along those sub-paths can lead to redundancy in the information as they relate to the same original trip. Thus, right selection of un-correlated sub-paths is crucial in the OD estimation problem. Although sub-paths (sequence of links) are similar to links in terms of unknown trip ends, they can capture trip distribution better than the point-based link flows. Thus, any extra information related to trip distribution in the objective function tends to improve the quality of OD estimate. The major contribution of this research is the novel consideration of the structural information from sub-path flows in the upper level objective function formulation. The study defines the structure of sub-path flows vector as "the arrangement of and the correlation that exist between the sub-path flows". The objective function is differentiable (if the mapping relationships for link flows and sub-path flows to OD flows are assumed locally constant), and the bi-level optimization can be achieved using gradient decent algorithm. The proposed methodology also relaxes the requirement of the known penetration rate of the vehicles providing the sub-path flow information.

The proposed methodology is generic and for ease of presentation, a network of Bluetooth MAC Scanner (BMS) based sub-path flow information is considered in this paper. The methodology is thoroughly tested on a simulation model from Brisbane, Australia.

The remainder of the paper is structured as follows: Section II describes the notations of terms used in this study; Section III discusses the proposed methodology; Section IV focusses on the experiments and results; Section V discusses the results of experiments; and finally the study concludes in Section VI with future study recommendations.

II. Notations of the terms

In order to describe the formulations relevant to this paper, the following mathematical notations are used.

- $\mathcal{A}$ denotes selected links of the study network; $\tilde{y}_a$ and y_a represent observed (say, from loop detectors) and simulated traffic counts/link flows on link $a \in \mathcal{A}$. $\tilde{\mathbf{y}} \in R^{|\mathcal{A}|}$ and $\mathbf{y} \in R^{|\mathcal{A}|}$ denote vectors of observed and simulated link flows, respectively.
- $\mathcal{H}$ represents the set of complete vehicle trajectories in a study network. $\mathcal{B}$ denotes set of sub-paths and $\mathcal{L}$ represent the total set of sub-trajectories (say, as sequence of BMS IDs) along $|\mathcal{B}|$ sub-paths. If the study performs analysis on only a random sample of sub-trajectories ($\tilde{\mathcal{L}}$), then we define $\eta = |\tilde{\mathcal{L}}|/|\mathcal{L}|$. η_b is used to represent the penetration rate of observed vehicle trajectories on b^{th} sub-path. $\boldsymbol{\eta} \in R^{|\mathcal{B}|}$ is vector representing market penetration rates of observed trips on $|\mathcal{B}|$ sub-paths.
- D denotes days of similar travel patterns. s_b^*, $\tilde{s}_{b,d}$, $\tilde{s}_b$ and s_b represent actual, observed (say, from Bluetooth) on d^{th} day ($d \in \mathbb{N}^{|D|}$), consolidated observations over $|D|$ days, and simulated sub-path flows on a sub-path $b \in \mathcal{B}$, respectively. $\mathbf{s}^* \in R^{|\mathcal{B}|}$, $\tilde{\mathbf{s}}_\mathbf{d} \in R^{|\mathcal{B}|}$, $\tilde{\mathbf{s}} \in R^{|\mathcal{B}|}$ and $\mathbf{s} \in R^{|\mathcal{B}|}$ denote vectors of actual, observed (on d^{th} day), observed (consolidated over $|D|$ days), and simulated sub-path

flows, respectively. $\boldsymbol{\mu}_{\mathbf{s}^*} \in R^{|\mathcal{B}|}$ is a vector with each cell value equal to mean of flow values in $\mathbf{s}^*$, and similarly $\boldsymbol{\mu}_{\tilde{\mathbf{s}}} \in R^{|\mathcal{B}|}$, $\boldsymbol{\mu}_{\mathbf{s}} \in R^{|\mathcal{B}|}$ correspond to $\tilde{\mathbf{s}}$ and $\mathbf{s}$, respectively.

- W denotes the set of OD pairs in the study network. x_w represents the number of estimated non-negative trips (by car) for OD pair $w \in W$, and similarly $\tilde{x}_w$ and ${x^*}_w$ are for prior and true OD flows. $\mathbf{x} \in R^{|W|}$, $\tilde{\mathbf{x}} \in R^{|W|}$, and $\mathbf{x}^* \in R^{|W|}$ denote estimated, prior, and true OD vectors, respectively. $\boldsymbol{\mu}_{\mathbf{x}} \in R^{|W|}$ is a vector with each cell value equal to mean of $\mathbf{x}$. Similarly $\boldsymbol{\mu}_{\tilde{\mathbf{x}}} \in R^{|W|}$ and $\boldsymbol{\mu}_{\mathbf{x}^*} \in R^{|W|}$correspond to $\tilde{\mathbf{x}}$ and $\mathbf{x}^*$, respectively.
- p_w^a is proportion of trips between w^{th} OD pair passing through link a. $\mathbf{P} \in R^{|\mathcal{A}|\times|W|}$ represents the link proportion matrix.
- q_w^b is proportion of trips between w^{th} OD pair passing through sub-path b. $\mathbf{Q} \in R^{|\mathcal{B}|\times|W|}$ represents the sub-path proportion matrix.

III. Proposed Methodology

The proposed methodology is illustrated in Fig.2. The new upper level formulation ($Z(\mathbf{x})$) includes two objectives: one based on traffic counts ($\tilde{\mathbf{y}}$ and $\mathbf{y}$) and other based on sub-path flows ($\tilde{\mathbf{s}}$ and $\mathbf{s}$). Details into the development of the objective function formulation, method of gradient-based OD estimation, procedure to implement the proposed approach, and development of Bluetooth based sub-path flows are presented in Section III.A, Section III.B, Section III.C, and Section III.D, respectively.

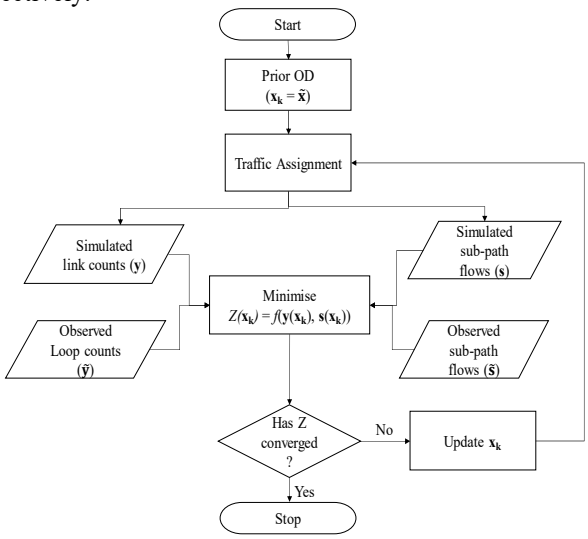

Fig. 2: Generic OD estimation algorithm based on the proposed approach

A. Proposed objective function formulation

The study assumes that the structural differences between observed ($\tilde{\mathbf{s}}$) and simulated ($\mathbf{s}$) sub-path flows can be used as proxy for the structural differences between the actual ($\mathbf{x}^*$) and estimated ($\mathbf{x}$) OD vectors. The structural deviations between the sub-path flows can be quantified using Pearson correlation coefficient (ρ). A higher correlation implies that both vectors (i. e. $\mathbf{s}$ and $\tilde{\mathbf{s}}$) are structurally closer to each other. This concept is borrowed from bio-medical analytics discipline where models with high dimensional data points are updated using similarity measures such as correlation coefficient [31].

The new upper-level formulation can be expressed in terms of the deviation between the observed ($\tilde{\mathbf{y}}$) and estimated ($\mathbf{y}$) link flows and the structural comparison between observed ($\tilde{\mathbf{s}}$) and simulated ($\mathbf{s}$) sub-path flows as shown in Equation 3.

$$\min_{\mathbf{x}} Z(\mathbf{x}) = \min_{\mathbf{x}} \tfrac{1}{2}\left(c_1 + (\mathbf{y}-\tilde{\mathbf{y}})^{\mathrm{T}}(\mathbf{y}-\tilde{\mathbf{y}})\right)\left(c_2 + f(\mathbf{s},\tilde{\mathbf{s}})\right)^{\mathrm{T}}\left(c_2 + f(\mathbf{s},\tilde{\mathbf{s}})\right) \quad (3)$$

$$f(\mathbf{s},\tilde{\mathbf{s}}) = \frac{1-\rho(\mathbf{s},\tilde{\mathbf{s}})}{2} \quad (3a)$$

$$\text{such that } \mathbf{y} = \mathbf{P}\mathbf{x}\ ;\ \mathbf{s} = \mathbf{Q}\mathbf{x} \quad (3b)$$

$$\rho(\mathbf{s},\tilde{\mathbf{s}}) = \frac{(\tilde{\mathbf{s}}-\boldsymbol{\mu}_{\tilde{\mathbf{s}}})^{\mathrm{T}}(\mathbf{s}-\boldsymbol{\mu}_{\mathbf{s}})}{\sqrt{(\tilde{\mathbf{s}}-\boldsymbol{\mu}_{\tilde{\mathbf{s}}})^{\mathrm{T}}(\tilde{\mathbf{s}}-\boldsymbol{\mu}_{\tilde{\mathbf{s}}})}\sqrt{(\mathbf{s}-\boldsymbol{\mu}_{\mathbf{s}})^{\mathrm{T}}(\mathbf{s}-\boldsymbol{\mu}_{\mathbf{s}})}} \quad (3c)$$

The second objective, $f(\mathbf{s},\tilde{\mathbf{s}}) = c_2 + \frac{1-\rho(\mathbf{s},\tilde{\mathbf{s}})}{2}$, considers any structural differences between the estimated/simulated and observed trip distribution from the perspective of sub-path flows. This acts as a scaling factor to the original traffic counts-based objective. Here, the similarity measure ($\rho(\mathbf{s},\tilde{\mathbf{s}})$) is converted to a dissimilarity measure ($\frac{1-\rho(\mathbf{s},\tilde{\mathbf{s}})}{2}$) with the addition of a constant "c" for stability.

This implies, when $\rho(\mathbf{s}, \tilde{\mathbf{s}}) = 1$, $Z(\mathbf{x})$ is multiplied by a factor of c^2 and for $\rho(\mathbf{s}, \tilde{\mathbf{s}}) = -1$, $Z(\mathbf{x})$ is scaled up $(c+1)^2$ times.

What should be the value of c_2? Ideally, $c_2 + \left(\frac{1-\rho(\mathbf{s},\tilde{\mathbf{s}})}{2}\right) \neq 0$

a) When structures of $\mathbf{s}$ and $\tilde{\mathbf{s}}$ are same then $\rho(\mathbf{s}, \tilde{\mathbf{s}})$ is equal to 1 and $\left(c + \frac{1-\rho(\mathbf{s},\tilde{\mathbf{s}})}{2}\right) \Rightarrow c$. Here, the objective function, $Z(\mathbf{x})$, is multiplied by a factor of ${c_2}^2$. Therefore, c_2=0 should not be considered as it will make the objective function zero.

b) When structures of $\mathbf{s}$ and $\tilde{\mathbf{s}}$ are extremely opposite then $\rho(\mathbf{s}, \tilde{\mathbf{s}})$ is equal to -1 and $\left(c_2 + \frac{1-\rho(\mathbf{s},\tilde{\mathbf{s}})}{2}\right) \Rightarrow (c_2 + 1)$. Here, the objective function, $Z(\mathbf{x})$ is multiplied by a factor of $(c_2+1)^2$. Therefore, c_2=-1 should not be considered as it will make the objective function zero.

For the current study we consider c_2=1. In this case,

a) When the structures of $\mathbf{s}$ and $\tilde{\mathbf{s}}$ are same then $Z(\mathbf{x})$ reduces to a traditional link counts deviation; that is, $\frac{1}{2}(\mathbf{y}-\tilde{\mathbf{y}})^{\mathrm{T}}(\mathbf{y}-\tilde{\mathbf{y}})$. This implies that simulated trip distribution matches the actual trip distribution, and simply minimizing traffic counts deviations should be sufficient to estimate OD.

b) When the structures of $\mathbf{s}$ and $\tilde{\mathbf{s}}$ are extremely opposite, the objective function multiplies $(2)^2$ times and becomes $2(\mathbf{y}-\tilde{\mathbf{y}})^{\mathrm{T}}(\mathbf{y}-\tilde{\mathbf{y}})$. This implies that deviation between traffic counts are amplified considering the extreme variations in the sub-path flows.

B. Gradient-based method for optimization of the objective function

The gradient descent optimization method is used to iteratively update $\mathbf{x}$. The updating step is based on two major factors: search direction and step-size (λ):

a) The search direction is determined by the gradient of $Z(\mathbf{x})$
   ∘The step-size (λ) parameter determines the number of

iterations required for the convergence. Lower values of λ ensure that the path of the gradient is smooth but computationally expensive. Higher values of λ can lead to higher values of the objective function, and the convergence could be affected.

Assuming **P** and **Q** are locally constant, the functions involved in Equation 3 are differentiable with respect to **x** and its gradient is expressed as shown in Equation 4 and 4a.

$$\frac{\partial Z(\mathbf{x})}{\partial \mathbf{x}} = \frac{\partial\left(\left((\mathbf{y}-\tilde{\mathbf{y}})\left(\mathrm{c}+\frac{1-\rho(\mathbf{s},\tilde{\mathbf{s}})}{2}\right)\right)^{T}\left((\mathbf{y}-\tilde{\mathbf{y}})\left(\mathrm{c}+\frac{1-\rho(\mathbf{s},\tilde{\mathbf{s}})}{2}\right)\right)\right)}{\partial \mathbf{x}} \tag{4}$$

$$= \left(\left(\mathrm{c}+\frac{1-\rho(\mathbf{s},\tilde{\mathbf{s}})}{2}\right)\mathbf{P}^{\mathrm{T}} - \frac{1}{2}\frac{\boldsymbol{\partial}\left(\rho(\mathbf{s},\ \tilde{\mathbf{s}})\right)}{\boldsymbol{\partial}\mathbf{x}}(\mathbf{y}-\tilde{\mathbf{y}})^{\mathrm{T}}\right)\left((\mathbf{y}-\tilde{\mathbf{y}})\left(\mathrm{c}+\frac{1-\rho(\mathbf{s},\tilde{\mathbf{s}})}{2}\right)\right) \tag{4a}$$

using $\mathbf{y} = \mathbf{Px}$

Using the mapping relationship (**Q**) between **s** and **x**, Equation 3b can be simplified as shown in Equation 5.

$$\begin{aligned}&\rho(\mathbf{Qx},\tilde{\mathbf{s}})\\ &= \frac{(\tilde{\mathbf{s}}-\boldsymbol{\mu}_{\tilde{\mathbf{s}}})^{\mathrm{T}}(\mathbf{Qx}-\boldsymbol{\mu}_{\mathbf{Qx}})}{\sqrt{(\tilde{\mathbf{s}}-\boldsymbol{\mu}_{\tilde{\mathbf{s}}})^{\mathrm{T}}(\tilde{\mathbf{s}}-\boldsymbol{\mu}_{\tilde{\mathbf{s}}})}\sqrt{(\mathbf{Qx}-\boldsymbol{\mu}_{\mathbf{Qx}})^{\mathrm{T}}(\mathbf{Qx}-\boldsymbol{\mu}_{\mathbf{Qx}})}}\\ &= \frac{\Gamma_1}{\sqrt{\Gamma_2}\sqrt{\Gamma_3}}\end{aligned} \tag{5}$$

Where,

$$\Gamma_1 = (\tilde{\mathbf{s}}-\boldsymbol{\mu}_{\tilde{\mathbf{s}}})^{\mathrm{T}}(\mathbf{Qx}-\boldsymbol{\mu}_{\mathbf{Qx}}); \tag{5a}$$
$$\Gamma_2 = (\tilde{\mathbf{s}}-\boldsymbol{\mu}_{\tilde{\mathbf{s}}})^{\mathrm{T}}(\tilde{\mathbf{s}}-\boldsymbol{\mu}_{\tilde{\mathbf{s}}}); \tag{5b}$$
$$\Gamma_3 = (\mathbf{Qx}-\boldsymbol{\mu}_{\mathbf{Qx}})^{\mathrm{T}}(\mathbf{Qx}-\boldsymbol{\mu}_{\mathbf{Qx}}). \tag{5c}$$

Now, $\frac{\partial\rho(\mathbf{Qx},\tilde{\mathbf{s}})}{\partial \mathbf{x}}$ can be expressed as shown in Equation 6.

$$\frac{\partial\rho(\mathbf{Qx},\tilde{\mathbf{s}})}{\partial \mathbf{x}} = \frac{\mathbf{Q}^{\mathrm{T}}\left((\tilde{\mathbf{s}}-\boldsymbol{\mu}_{\tilde{\mathbf{s}}}) - \frac{\Gamma_1}{\Gamma_3}(\mathbf{Qx}-\boldsymbol{\mu}_{\mathbf{Qx}})\right)}{\sqrt{\Gamma_2}\sqrt{\Gamma_3}} \tag{6}$$

Thus, the differential objective function provides opportunities to consider standard gradient based method to update the OD vector; that is, during any k[th] iteration $\mathbf{x_k}$ is updated to $\mathbf{x_{k+1}}$ using the search direction and optimal step-size as expressed in the Equation 7. Here, $Z(\mathbf{x})$ and $\mathbf{x}$ in $\frac{\partial Z(\mathbf{x})}{\partial \mathbf{x}}$ refer to the values corresponding to k[th] iteration; *e* is vector of 1s and of dimension same as **x**; and Hadamard product "∘" is used for element wise multiplication between λ_k and the gradient, and $\mathbf{x_k}$ and $\left(e-\lambda_k\circ\frac{\partial Z(\mathbf{x})}{\partial \mathbf{x}}\right)$.

$$\mathbf{x}_{\mathrm{k+1}} = \mathbf{x}_{\mathrm{k}}\circ\left(e-\lambda_k\circ\frac{\partial Z(\mathbf{x})}{\partial \mathbf{x}}\right) \tag{7}$$

$$\lambda_k\circ\frac{\partial Z(\mathbf{x})}{\partial \mathbf{x}} < 1 \tag{7a}$$

C. Procedure to implement the proposed methodology

To execute the framework illustrated in Fig. 2 under controlled environment, we need to run upper-level and lower optimizations one after another in an integrated manner. The step by step procedure for which is outlined below:

- Step-0: Obtain the observed sub-path flows (**$\tilde{\mathbf{s}}$**) and observed link flows (**$\tilde{\mathbf{y}}$**).
- Step-1: Set *k=1*; $\mathbf{x_k} = \tilde{\mathbf{x}}$.
- Step-2: Load the study network in Aimsun next [32] with demand, $\mathbf{x_k}$, and run traffic assignment (either stochastic route choice (SRC) assignment or dynamic user equilibrium). The outputs of the simulation are link flows($\mathbf{y_k}$), sub-path flows ($\mathbf{s_k}$), link-proportion matrix ($\mathbf{P_k}$) and sub-path proportion-matrix ($\mathbf{Q_k}$).
- Step-3: Minimise the objective function, *Z(***x***)* with respect to $\mathbf{x_k}$ (refer Equation 3).
- Step-4: Check for termination criterion, and if it is not met, set *k* := *k+1*; update the demand ($\mathbf{x_k}$) for the next iteration (refer Equation 7), and go to Step 2. Else terminate the optimisation, and value of $\mathbf{x_k}$ is the final estimated OD vector.

The termination criterion can be either based on maximum relative change in the elements of estimated OD flows at successive iterations [1] or observed convergence for a fixed number of iterations [8].

For the current analysis, the codes for the optimisation are written in MATLAB (2017 version), and lower level traffic assignment is optimised using Aimsun next [32]. We have used the default parameter values for both demand scenarios and experiments in Aimsun. A Python script is written to integrate the optimisation model (in MATLAB) with the traffic assignment (in Aimsun). However, MATLAB is the primary platform that writes OD data into Aimsun OD format, runs the simulation, executes the Python script, and reads the simulation outputs for further optimisation process. The integration of both platforms is further shown in Fig. 3. This integration of Aimsun with Matlab is similar to the one presented in Antoniou et al., [18].

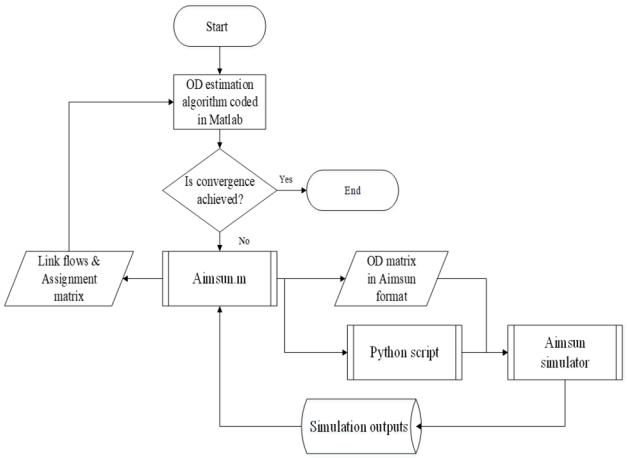

Fig. 3: Matlab-Aimsun next integration framework

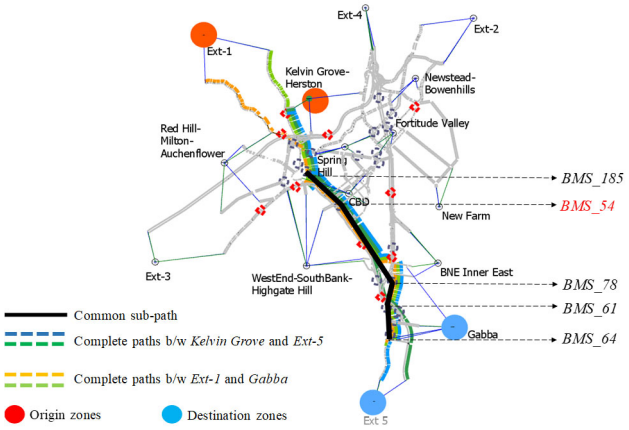

Fig. 4: Complete path vs Bluetooth sub-path

The aforementioned sections demonstrate that an additional objective based on sub-path flows can be incorporated into bi-level formulation. The next section discusses the development of sub-path flows from the network of Bluetooth MAC scanners (BMS).

D. Bluetooth sub-path flows

We assume that the road network is equipped with Bluetooth MAC Scanners (BMS) [33]. For instance, in Brisbane, Australia we have over 1200 BMSs monitoring traffic on the Brisbane City Council (BCC) region[34]. The data from these network of BMSs can be integrated to define the trajectories of the Bluetooth vehicles [35] and the corresponding paths.

These paths inferred from BMS detections are only sub-paths of actual paths traversed by vehicles. This is because, a) not all Bluetooth equipped vehicles are detected at the scanning zone; and b) the entire network is not fully equipped with the BMS, and the origin/destination BMS for the Bluetooth vehicle trajectory might not truly correspond to the true origin/destination zone for the network for which the OD is estimated.

For ease of understanding, refer to Fig. 4 that illustrates the difference between complete paths and a sub-path. The complete paths between the OD pairs Kelvin Grove-Ext-5, and Ext-1-Gabba share a common subpath that can be represented as a sequence of BMS – 185-78-61-64. Note that the BMS_54 is not in the sequence due to missed detection. Thus, it can be seen that it is not possible to infer the true trip ends (i.e. Ext-1 or Kelvin Grove and Ext-5 or Gabba) from the above sub-path.

Sometimes, a set of sub-paths can belong to the same trip due to missed detections during the course of travel. In such cases the trips along those sub-paths can lead to redundancy in the information as they relate to the same original trip. Thus, right selection of un-correlated sub-paths is crucial in the OD estimation problem.

The penetration rate of Bluetooth based counts at a specific level can range from 10%-30% [29]. However, the penetration rate for the observed path flows from BMS can be much lower say, around 5% ([36] reported 4.4% average detection rate for 12 OD pairs at an interchange level) and can vary over different paths. We address this issue as follows: We propose to generate a sub-path flow vector by combining sub-path flows observed from several days of similar travel patterns. For instance, the observed sub-path flows from $|D|$ regular working Mondays can be used to develop a consolidated vector of observed sub-path flows for a typical working Monday. Thus, $\tilde{s}_b$ can be considered as a consolidation of several observations of Bluetooth flows on sub-path b as shown in Equation 8.

$$\tilde{s}_b = \sum_{d=1}^{d=|D|} \tilde{s}_{b,d} \tag{8}$$

The consolidated vector $\tilde{\mathbf{s}}$ can then be expressed as shown in Equation 9.

$$\tilde{\mathbf{s}} = \sum_{d=1}^{d=|D|} \tilde{\mathbf{s}}_{\mathbf{d}} \tag{9}$$

IV. Experiments and Results

A. Study network

To test the proposed methodology, the study network should have the following properties:

1. It should be realistic and representative of the existing infrastructure;
2. It should have sufficient route choice options;
3. It should have a combination of at least two different types of road hierarchy i.e. motorway and arterial;
4. OD pairs should have sufficient overlap between the paths;
5. It should have sufficient Bluetooth connectivity; that is, the subpaths should be along the major routes; and
6. Loop detectors to be located on important corridors.

The study network meeting the above-mentioned criteria is presented in Fig. 5. It represents the core of the Brisbane city network imported into Aimsun next [32] from open street map [37]. The network comprises of 15 centroids (zones), 24 loop

detectors (red squares in Fig. 5), and 20 Bluetooth scanners (blue circles in Fig. 5) and 5 external zones. The loop detectors and BMS are placed on the major roadways such as Pacific Motorway, Clem Jones Tunnel, Coronation Drive, Inner City Bypass, and Kelvin Grove Road etc.

The OD matrix is designed at a zonal level equivalent to Statistical Area 2 (SA2) [38] and is 15 x 15 in size. Internal trips are excluded in the analysis. Since, the number of OD pairs is greater than 200 it is a high dimensional OD matrix [39]. The 15 zonal centroids shown are:

- West End-South Bank-Highgate Hill;
- Gabba;
- Brisbane (BNE) Inner East;
- New Farm;
- Fortitude Valley;
- Spring Hill;
- Central Business District (CBD);
- Newstead-Bowen Hills;
- Kelvin Grove–Herston;
- Red Hill–Milton–Auchenflower;
- Five external zonal centroids; that is, Ext-1, Ext-2, Ext-3, Ext-4, and Ext-5, respectively.

The traffic from each zone is loaded into to the network through a number of connectors. The zones, namely Ext-1, Ext-2, Ext-3, Ext-5 and New Farm have 2 connectors each; Ext-4, Kelvin Grove, Newstead-Bowen hills and BNE Inner East have 3 each; West End-South bank- Highgate Hill, Red Hill-Milton-Auchenflower, Fortitude Valley, and Gabba have 4 each; and Brisbane CBD has 5 connectors, respectively. The number of paths per OD pair are chosen to be greater than one, and the paths connecting different OD pairs have sufficient overlap. Refer to Fig. 6 for multiple (6 paths) and overlapping route choice options between the OD pair - Kelvin Grove-Herston to Ext-5.

Each zone/centroid is connected by one or more than one BMS so that complete path can be identified as a sequence of BMS IDs between any OD pair. Although complete trajectories are available in the simulation, the analysis in this study is performed using Bluetooth sub-paths only. Refer Section IV.B for more details.

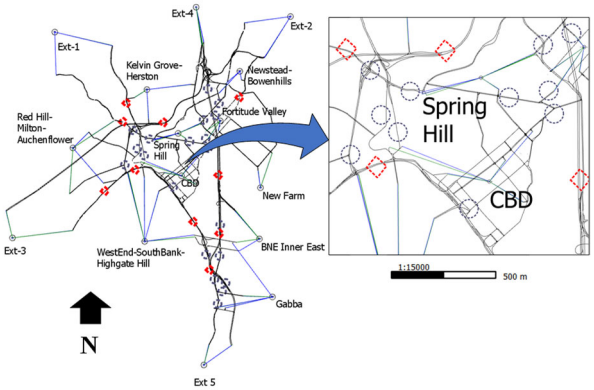

Fig. 5: Study site with Bluetooth scanners (dotted circles) and Loop detectors (dotted rectangles)

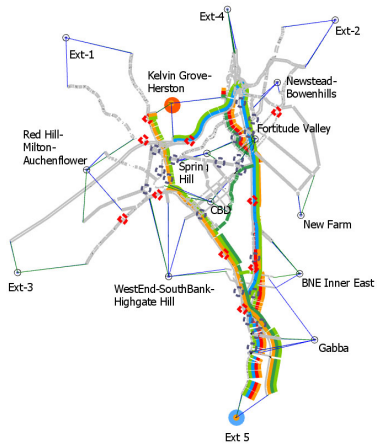

Fig. 6: Demonstration of route choice options between the OD pair - Kelvin Grove-Herston to Ext-5

B. Design of Experiments

For the current analysis we aim to estimate typical OD for the network, given data from several days. For instance, we are interested in typical OD during morning peak hours of regular Monday using loop detector and BMS data from several regular Mondays. To generate synthetic data for such application we do the following:

a) Define number of similar OD matrices representing normal day-to-day travel demand variability. The average of these OD represents the typical OD and is the ground truth for the study. The details are presented in Section IV.B.1).

b) Simulate the traffic with an OD and export the loop and Bluetooth data. Repeat this process over all the defined ODs. This provides database for individual day loop counts and BMS based sub-path flows (refer Section IV.B.3).

1) Defining similar OD matrices

For the study network, we develop a database of OD matrices that are structurally similar to each other. Here, we define a typical OD matrix $\mathbf{x}^*$ (one hour demand equal to 6736 trips) and generate additional four similar OD matrices by randomly perturbing $\mathbf{x}^*$ with a standard deviation of 5%. Refer Fig. 7 for matrix version of $\mathbf{x}^*$. The OD matrices are denoted by $\mathbf{x_i}^*$, where $\mathbf{x_1}^* = \mathbf{x}^*$ and $\mathbf{x_i}^* = \text{rand}(\mathbf{x}^*, 5\%)\ \forall\ 2 \leq i \leq 5$ such that $x_{w,i}{}^* > 0$.

Zones	Origin \ Dest	Z1	Z2	Z3	Z4	Z5	Z6	Z7	Z8	Z9	Z10	Z11	Z12	Z13	Z14	Z15
Ext1	Z1	0	60	40	30	60	10	20	30	44	50	20	20	40	44	40
Kelvin Grove-Herston	Z2	60	0	10	20	24	26	28	40	38	34	16	10	20	38	56
Red Hill-Milton-Auchen Flower	Z3	40	10	0	50	20	16	20	40	20	10	20	4	8	20	40
Ext 3	Z4	30	20	50	0	6	20	24	26	28	40	38	8	16	28	48
WestEnd-SouthBank-Highgate Hill	Z5	60	24	20	6	0	30	44	50	20	16	20	20	40	20	88
Ext 5	Z6	10	26	16	20	30	0	20	50	20	16	20	20	40	20	40
Gabba	Z7	20	28	20	24	44	20	0	30	44	50	20	20	40	44	30
BNE Inner East	Z8	30	40	40	26	50	50	30	0	6	20	24	28	56	6	60
New Farm	Z9	44	38	20	28	20	20	44	6	0	30	44	20	40	30	88
Newstead-Bowen Hills	Z10	50	34	10	40	16	16	50	20	30	0	4	20	40	30	100
Ext2	Z11	20	16	20	38	20	20	20	24	44	4	0	20	40	44	40
Ext4	Z12	20	10	4	8	20	20	20	28	20	20	20	0	30	20	40
Fortitude Valley	Z13	40	20	8	16	40	40	40	56	40	40	40	30	0	30	80
Spring Hill	Z14	44	38	20	28	20	20	44	6	30	30	44	20	30	0	88
CBD	Z15	40	56	40	48	88	40	30	60	88	100	40	40	80	88	0

Fig 7: Matrix version of true OD vector (x*) used for the study region

2) Traffic Simulation

For the current analysis, one hour (7: 30 AM- 8:30 AM) simulation is performed using Aimsun micro- which is a

stochastic simulation at the microscopic level. The assignment model considered is stochastic route choice. The demand for each simulation is defined as per Section IV.B.1) resulting in five different scenarios for a typical OD. For each scenario five replications are simulated. Each replication has its own random seed, resulting in a simulation with different random selection of the stochastic parameters.

3) Traffic database (Loops and BMS)

The traffic database consists of loops and Bluetooth records from a total of 25 simulation runs (5 similar demand patterns and 5 replications for each demand). Refer Fig. 8 that explains the process of generating $\tilde{\mathbf{s}}$ and $\tilde{\mathbf{y}}$.

The network has 24 loop detectors (see Fig. 5). Total vehicle counts at each detector location during each simulation run is obtained. Finally traffic count at each detector location is defined by average of the counts at the location from 25 simulations.

The network has 20 BMSs (see Fig. 5) that detects Bluetooth equipped vehicles. Interested readers can refer to the traffic and communication simulation model for simulating BMS dataset using Aimsun [33]. In this study, the sub-paths are pre-selected before conducting the analysis. The number of common sub-paths in all 25 simulation runs is identified to be $|\mathcal{B}|$=113. For the analysis we have considered four different cases with Bluetooth penetration rates (see Section IV.B.4). Bluetooth sub-path trajectories are estimated independently for each case.

The process of generating $\tilde{\mathbf{y}}$ and $\tilde{\mathbf{s}}$ illustrated in Fig. 8 is briefly explained as follows:

- First, initiate $\tilde{\mathbf{y}}_{i,r}$ and $\tilde{\mathbf{s}}_{i,r}$ of dimensions $|\mathcal{A}|$ x 1 = 24 x 1 and $|\mathcal{B}|$ x 1=113 x 1, respectively for i^{th} OD matrix ($\mathbf{x}_i^*$) and r^{th} replication with zero flow values.
- Second, simulated traffic counts from $|\mathcal{A}|$=24 loops are denoted by $\tilde{\mathbf{y}}_{i,r}$. The database of vehicle trajectories are stored as a complete sequence of BMS in $\mathcal{H}_{i,r}$. The first and last BMSs of each complete trajectory sequence are directly linked to the actual origin and destination zones of the simulated trip.
- Third, convert $\mathcal{H}_{i,r}$ to sub-trajectories ($\mathcal{L}_{i,r}$) by de-selecting a few scanner IDs from the beginning and ending of the complete trajectory sequence (this is done because the actual Bluetooth trajectories do not always represent true trip ends) and due to the deselection process $|\mathcal{L}_{i,r}|$ is less than $|\mathcal{H}_{i,r}|$. For instance, $|\mathcal{H}_{1,1}|$=5,273 and $|\mathcal{L}_{1,1}|$=3,875 in our study.
- Fourth, identify η percent of sub-trajectories ($\tilde{\mathcal{L}}_{i,r}$) from the set $\mathcal{L}_{i,r}$. For instance, $|\tilde{\mathcal{L}}_{1,1}|$=97 for $\eta\% = 2.5\%$ of 3,875 of total sub-trajectories.
- Fifth, count the number of sub-trajectories (from $\tilde{\mathcal{L}}_{i,r}$) passing through each sub-path in $\mathcal{B}$ and add it to $\tilde{\mathbf{s}}_{i,r}$. Note that η% random selection in the previous step might not account all subpaths, and in such cases, some of the subpaths can contain zero flow values in $\tilde{\mathbf{s}}_{i,r}$. For instance, $|\tilde{\mathcal{L}}_{1,1}|$=97 sub-trajectories (for $\eta\% = 2.5\%$) resulted in only 44 out of $|\mathcal{B}|$ = 113 sub-paths, which means the flows for the rest are zeros.
- Repeat steps from first to fifth for all 25 simulations (i.e. i=1 to 5 and r=1 to 5). The average traffic counts observations are obtained as $\tilde{\mathbf{y}} = \frac{\sum_{i=1}^{5}\sum_{r=1}^{5}\tilde{\mathbf{y}}_{i,r}}{25}$ and the final consolidated vector of subpath flows is obtained as $\tilde{\mathbf{s}} = \sum_{i=1}^{5}\sum_{r=1}^{5}\tilde{\mathbf{s}}_{i,r}$.

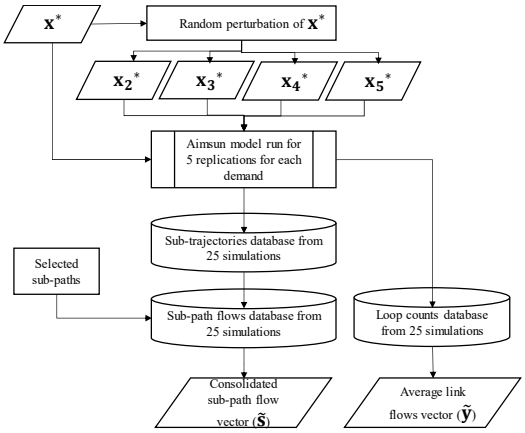

Fig. 8: Method to generate synthetic data ($\tilde{\mathbf{y}}$ and $\tilde{\mathbf{s}}$)

4) Experiment cases

To evaluate the impact of the Bluetooth penetration rate we consider different scenarios as follows:

a) *Traditional case:* $Z(\mathbf{x})$ is expressed only in terms of traffic counts deviations (Equation 1). No Bluetooth based sub-path trajectories are considered.
b) *Case-1:* Here, $\tilde{\mathbf{s}}$ is generated using $\eta\% = 2.5\%$ and $Z(\mathbf{x})$ is expressed using Equation 3.
c) *Case -2:* Here, $\tilde{\mathbf{s}}$ is generated using $\eta\% = 5\%$ and $Z(\mathbf{x})$ is expressed using Equation 3.
d) *Case -3:* Here, $\tilde{\mathbf{s}}$ is generated using $\eta\% = 7.5\%$ and $Z(\mathbf{x})$ is expressed using Equation 3.
e) *Case -4:* Here, $\tilde{\mathbf{s}}$ is generated using $\eta\% = 10\%$ and $Z(\mathbf{x})$ is expressed using Equation 3.

C. Performance evaluation

To check the efficiency of the proposed methodology, the final estimated OD ($\mathbf{x}$) individually for different cases is compared with ground truth, $\mathbf{x}^*$ using following two indicators

a) $\mathrm{RMSE}(\mathbf{x}, \mathbf{x}^*)$ (Equation 10): It is a standard measure to quantify average deviation of individual elements of the estimated OD vector (x_w) with that of ground truth ($x^*{}_w$). In the Equation 10, $|W|$ is the size of the OD vector.

$$\mathrm{RMSE}(\mathbf{x}, \mathbf{x}^*) = \sqrt{\frac{1}{|W|}\sum_{w\in W}(x_w - x^*{}_w)^2} \qquad (10)$$

b) $\rho(\mathbf{x}, \mathbf{x}^*)$ (Equation 11): This measure is more robust [19] and is used to compare only the structural deviation between the estimated OD matrix ($\mathbf{x}$) and ground truth OD vector ($\mathbf{x}^*$). Notations of terms used in Equation 11 are explained in Section II.

$$\rho(\mathbf{x}, \mathbf{x}^*) = \frac{(\mathbf{x}-\boldsymbol{\mu}_{\mathbf{x}})^{\mathrm{T}}(\mathbf{x}^*-\boldsymbol{\mu}_{\mathbf{x}^*})}{\sqrt{(\mathbf{x}-\boldsymbol{\mu}_{\mathbf{x}})^{\mathrm{T}}(\mathbf{x}-\boldsymbol{\mu}_{\mathbf{x}})}\sqrt{(\mathbf{x}^*-\boldsymbol{\mu}_{\mathbf{x}^*})^{\mathrm{T}}(\mathbf{x}^*-\boldsymbol{\mu}_{\mathbf{x}^*})}} \qquad (11)$$

D. A Priori OD matrix for optimization

To test the robustness of the proposed methodology with respect to the consideration of the *a priori* OD matrix for optimization, we perform the analysis independently on three different *a priori* OD matrices ($\tilde{\mathbf{x}}_1, \tilde{\mathbf{x}}_2$, and $\tilde{\mathbf{x}}_3$). Table I presents the quality of the priori OD matrix ($\tilde{\mathbf{x}}_c$) with respect to the ground-truth ($\mathbf{x}^*$), and are chosen such a way that the error values of the *a priori* matrices are in decreasing order while the structures are almost similar.

TABLE I
COMPARISON OF $\tilde{\mathbf{x}}_c$ WITH $\mathbf{x}^*$

Prior ODs ($\tilde{\mathbf{x}}_c$)	RMSE($\tilde{\mathbf{x}}_c, \mathbf{x}^*$)	$\rho(\tilde{\mathbf{x}}_c, \mathbf{x}^*)$
$\tilde{\mathbf{x}}_1$	14.02	0.8142
$\tilde{\mathbf{x}}_2$	13.24	0.8178
$\tilde{\mathbf{x}}_3$	12.34	0.7964

E. Results

In this section, we discuss the quality of the OD estimates ($\mathbf{x}$) resulted from different cases and consideration of different *a priori* OD matrices.

1) Quality assessment of OD estimates using RMSE ($\boldsymbol{x}, \boldsymbol{x}^*$)

Fig. 9 summarizes the results using RMSE as the performance indicator. Here, different link graph corresponds to different *a priori*-OD matrix. The x-axis represents different cases.

The results indicate a gradual improvement in the quality of $\mathbf{x}$ as measured through RMSE. For instance, the set of experiments initiated with $\tilde{\mathbf{x}}_1$ improved from RMSE ($\tilde{\mathbf{x}}_1, \mathbf{x}^*$) =14.02 to RMSE($\mathbf{x}, \mathbf{x}^*$) =11.34 (for $\eta\%$=10%). Similarly, the results for the experiments initiated with $\tilde{\mathbf{x}}_2$, and $\tilde{\mathbf{x}}_3$ have also demonstrated significant improvements.

The percent improvements in RMSE($\mathbf{x}, \mathbf{x}^*$) are illustrated in Fig. 10. The percent improvement is calculated with respect to $\tilde{\mathbf{x}}_c$, and we can observe greater improvements in all cases with higher error values of *a priori* increase. For example, at $\eta\%$=2.5%, there is 6.88% improvement (from RMSE ($\tilde{\mathbf{x}}_3, \mathbf{x}^*$) =12.36 to RMSE($\mathbf{x}, \mathbf{x}^*$) =11.50) as against 17.05% improvement (from RMSE ($\tilde{\mathbf{x}}_1, \mathbf{x}^*$) =14.02 to RMSE($\mathbf{x}, \mathbf{x}^*$) =11.63). However, the traditional case showed lesser improvement in RMSE as compared to other cases that are sub-path flows based objective function. The percentage RMSE improvement is only slightly improved from case-1 to case-4.

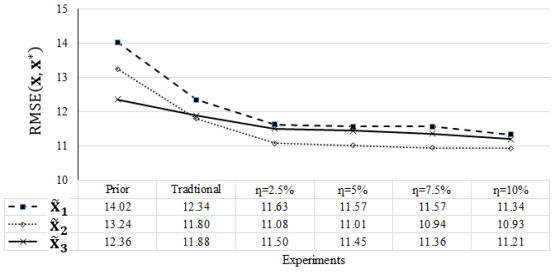

	Prior	Tradtional	η=2.5%	η=5%	η=7.5%	η=10%
$\tilde{\mathbf{x}}_1$	14.02	12.34	11.63	11.57	11.57	11.34
$\tilde{\mathbf{x}}_2$	13.24	11.80	11.08	11.01	10.94	10.93
$\tilde{\mathbf{x}}_3$	12.36	11.88	11.50	11.45	11.36	11.21

Fig 9: RMSE ($\tilde{\boldsymbol{x}}_c, \boldsymbol{x}^*$) vs $RMSE(\boldsymbol{x}, \boldsymbol{x}^*)$ for all experiments

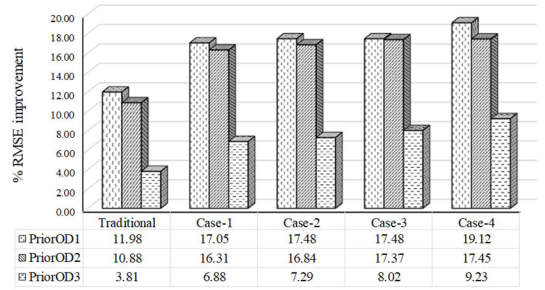

	Traditional	Case-1	Case-2	Case-3	Case-4
PriorOD1	11.98	17.05	17.48	17.48	19.12
PriorOD2	10.88	16.31	16.84	17.37	17.45
PriorOD3	3.81	6.88	7.29	8.02	9.23

Fig 10: Percentage improvements in $RMSE(\boldsymbol{x}, \boldsymbol{x}^*)$ with respect to RMSE ($\tilde{\boldsymbol{x}}_c, \boldsymbol{x}^*$)

2) Quality assessment of OD estimates using $\rho(\boldsymbol{x}, \boldsymbol{x}^*)$

The $\rho(\mathbf{x}, \mathbf{x}^*)$ results as shown in Fig. 11 demonstrate that there is structural improvement in the OD estimates as $\eta\%$ increases from 2.5% to 10%. Fig. 11 also highlights that the traditional traffic counts-based approach could not bring any significant structural improvements in the OD estimates unless additional information from Bluetooth sub-path flows is introduced.

The percent improvement in $\rho(\mathbf{x}, \mathbf{x}^*)$ is illustrated in Fig. 12. It can be seen that rates of improvement for sub-path flows based cases are better than that of traditional method. In the traditional case, the percentage improvement is negative for $\tilde{\mathbf{x}}_1$ based experiment, which implies a structural degradation, and simulation runs based on $\tilde{\mathbf{x}}_2$ and $\tilde{\mathbf{x}}_3$ have showed only little improvement. While, the percent improvement in $\rho(\mathbf{x}, \mathbf{x}^*)$ is higher for the rest (i.e. case-1 to case-4), there is no significant difference in the improvements within them.

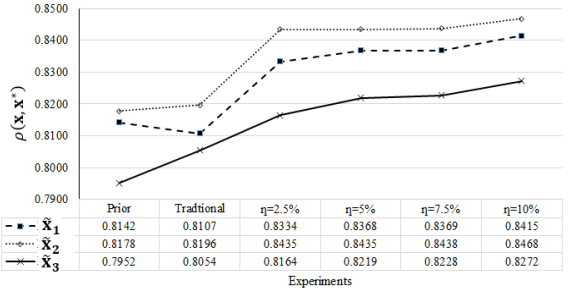

	Prior	Tradtional	η=2.5%	η=5%	η=7.5%	η=10%
$\tilde{\mathbf{x}}_1$	0.8142	0.8107	0.8334	0.8368	0.8369	0.8415
$\tilde{\mathbf{x}}_2$	0.8178	0.8196	0.8435	0.8435	0.8438	0.8468
$\tilde{\mathbf{x}}_3$	0.7952	0.8054	0.8164	0.8219	0.8228	0.8272

Fig 11: ρ ($\tilde{\boldsymbol{x}}_c, \boldsymbol{x}^*$) vs $\rho(\boldsymbol{x}, \boldsymbol{x}^*)$ for all experiments

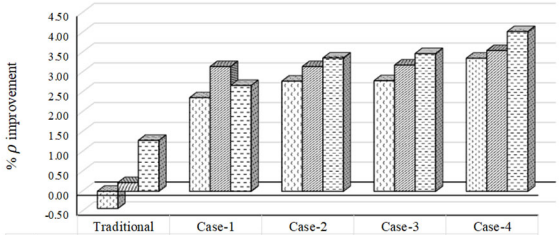

	Traditional	Case-1	Case-2	Case-3	Case-4
PriorOD1	-0.43	2.36	2.78	2.79	3.35
PriorOD2	0.22	3.14	3.14	3.18	3.55
PriorOD3	1.28	2.67	3.36	3.47	4.02

Fig 12: Percentage improvements in $\rho(\boldsymbol{x}, \boldsymbol{x}^*)$ with respect to $\rho(\tilde{\boldsymbol{x}}_c, \boldsymbol{x}^*)$

3) Statistical assessment of the results

The difference between the results obtained from traditional method and those from the cases with Bluetooth penetration rates are statistically compared at α=5% level of significance using paired t-test, and are shown in the Table II.

TABLE II
STATISTICAL DIFFERENCE BETWEEN TRADITIONAL AND REST OF THE CASES

	$\text{RMSE}(\mathbf{x}, \mathbf{x}^*)$		$\rho(\boldsymbol{x}, \boldsymbol{x}^*)$	
	t-value	p-value	t-value	p-value
Trad. vs Case-1	5.4012	0.0326	-4.6663	0.0430
Trad. vs Case-2	5.6788	0.0296	-7.6341	0.0167
Trad. vs Case-3	7.0463	0.0196	-8.4856	0.0136
Trad. vs Case-4	8.8218	0.0126	-10.1708	0.0095

Although, the improvements in the absolute values of both RMSE (Fig. 9 and Fig. 10) and ρ (Fig. 11 and Fig. 12) seem to be marginal, Table II demonstrates that that the absolute t-values are greater than the critical value (i.e. 3.182 for 3 degrees of freedom) at 95% confidence level, and thus the differences between traditional and Bluetooth sub-paths based results are statistically significant.

V. DISCUSSION

The goodness of fit measurements namely, $\text{RMSE}(\mathbf{x}, \mathbf{x}^*)$ and $\rho(\mathbf{x}, \mathbf{x}^*)$ showed significant improvement with respect to both *a priori* OD and traditional method even at lower penetration rates of Bluetooth trips (i.e. η%=2.5% consolidated over $|D|$=25 simulations). We can also see that the results for η% > 2.5% (i.e. case-2 to case-4) are better than η%=2.5% (case-1). However, in practice, the chances of η%=2.5% is higher than η% = 10%, and significant improvement in the results for case-1 demonstrated the practical significance of the proposed methodology. For instance, few samples of Bluetooth trajectories through key corridors that serve higher traffic demand such as, major arterials and motorways, should serve the purpose of enhancing the quality of OD estimates for large scale urban networks.

The traditional method did not show any significant structural enhancements (Fig. 11 and Fig. 12) although the $\text{RMSE}(\mathbf{x}, \mathbf{x}^*)$ measure is improved (Fig. 9 and Fig. 10). This shows that preserving the OD structure using additional path-based information from Bluetooth short trips (which we referred as sub-path flows in this paper) helps to direct OD convergence towards a better solution estimate instead of 'getting stuck' in the local optima. The trend of improvement in both $\text{RMSE}(\mathbf{x}, \mathbf{x}^*)$ and $\rho(\mathbf{x}, \mathbf{x}^*)$ is same for experiments that are based on Bluetooth sub-path flows and the difference among them is not very significant. This is because subpath flows with η%=2.5% observed from several days (25 in this study) of similar travel patterns amounts to 62.5% (i.e. 25*2.5%) of total Bluetooth trips. This significant rise in the consolidated sample rate is sufficient to cause considerable improvement even at daily market penetration rate of 2.5%.

The experiments are tested in a controlled environment due to the unavailability of the ground truth (i.e. true OD). Nevertheless, the study demonstrates that the proposed methodology is robust for different prior OD matrices and lower sample of random Bluetooth observations. The Brisbane City Council (BCC) and the Department of Transport Main Roads (TMR) have been recording the Bluetooth observations on a continuous basis, and it is possible to have the database of traffic observations from several days representing similar travel patterns [40]. Thus, the proposed methodology is ready for practical implementation on real world networks with trajectories and loop counts database.

VI. CONCLUSION

One of the major limitations of traffic counts-based OD estimation is the problem of under-determinacy, and due to which the quality of OD estimates cannot always be guaranteed. With the advancements in technology, many emerging data sources such as Bluetooth are able to provide additional travel related information such as vehicle trajectories. However, they are only partial observations of complete trips with random and unknown market penetration rates. Studies in the past have developed objective function based on partial path (referred as sub-path in this study) information but with an assumption that their penetration rate is known.

To this end, the study develops a new upper level formulation in the bi-level OD estimation problem that incorporates additional structural information of sub-path flows. The proposed sub-paths flows based approach maintains structural consistency in the OD matrix estimates and is better than traditional traffic counts-based technique. This is because the structure of Bluetooth sub-path flows, which is independent of the penetration rates, provides an additional higher-dimensional information about trip distribution as against point-based observations of link flows. The robustness of the proposed methodology, tested through several experiments, has demonstrated its practical relevance for situations when the penetration rate of Bluetooth trajectories is very low.

Although, the present study demonstrated results better than the traditional approach (as also observed from t-test results), the study can be extended in the following research directions. First, the solution algorithm that is adopted is still a classical gradient descent and the issue of "stuck at local minima" needs to be addressed. The step size is crucial in gradient descent algorithm and needs to be adjusted for different OD flow values. A stochastic gradient decent algorithm can introduce some randomness to escape from local minima in order to reach a better minimal value. Thus, as a continuation of the current study, we propose to test the methodology across different state-of-the-art optimization algorithms such as stochastic perturbation and simultaneous approximation (SPSA), Genetic Algorithms etc. Second, more experiments shall be conducted in future for different spatial coverages of Bluetooth sub-paths. Third, the current study is based on a synthetic network, and we would like to test it on a real case study network for the future study.

Although, the study demonstrated using Bluetooth sub-path flows, the proposed approach is generic in nature and the formulation holds good for path (partial/complete) flows observed from any other emerging data sources such as WIFY, GPS, mobile phone etc.

ACKNOWLEDGEMENTS

The authors are thankful to Queensland Department of Transport and Main Roads (TMR) and Queensland University of Technology for supporting this research. The conclusions of this paper reflect understandings of the authors, who are responsible for the accuracy of the research findings.

REFERENCES

[1] M. J. Maher, X. Zhang, and D. Van Vliet, "A bi-level programming approach for trip matrix estimation and traffic control problems with stochastic user equilibrium link flows," *Transportation Research Part B: Methodological,* vol. 35, pp. 23-40, 2001.

[2] G. Cantelmo, E. Cipriani, A. Gemma, and M. Nigro, "An adaptive bi-level gradient procedure for the estimation of dynamic traffic demand," *IEEE Transactions on Intelligent Transportation Systems,* vol. 15, pp. 1348-1361, 2014.

[3] H. J. Van Zuylen and L. G. Willumsen, "The most likely trip matrix estimated from traffic counts," *Transportation Research Part B: Methodological,* vol. 14, pp. 281-293, 1980.

[4] H. Spiess, "A maximum likelihood model for estimating origin-destination matrices," *Transportation Research Part B: Methodological,* vol. 21, pp. 395-412, 1987.

[5] M. Maher, "Inferences on trip matrices from observations on link volumes: a Bayesian statistical approach," *Transportation Research Part B: Methodological,* vol. 17, pp. 435-447, 1983.

[6] E. Cascetta, "Estimation of trip matrices from traffic counts and survey data: a generalized least squares estimator," *Transportation Research Part B: Methodological,* vol. 18, pp. 289-299, 1984.

[7] E. Cascetta, D. Inaudi, and G. Marquis, "Dynamic estimators of origin-destination matrices using traffic counts," *Transportation science,* vol. 27, pp. 363-373, 1993.

[8] M. Bullejos, J. Barceló Bugeda, and L. Montero Mercadé, "A DUE based bilevel optimization approach for the estimation of time sliced OD matrices," in *Proceedings of the International Symposia of Transport Simulation (ISTS) and the International Workshop on Traffic Data Collection and its Standardisation (IWTDCS), ISTS'14 and IWTCDS'14*, 2014.

[9] H. Spiess, "A gradient approach for the OD matrix adjustment problem," *CENTRE DE RECHERCHE SUR LES TRANSPORTS PUBLICATION,* vol. 1, p. 2, 1990.

[10] E. Cascetta and M. N. Postorino, "Fixed point approaches to the estimation of O/D matrices using traffic counts on congested networks," *Transportation science,* vol. 35, pp. 134-147, 2001.

[11] E. Cipriani, M. Florian, M. Mahut, and M. Nigro, "A gradient approximation approach for adjusting temporal origin–destination matrices," *Transportation Research Part C: Emerging Technologies,* vol. 19, pp. 270-282, 2011.

[12] H. Kim, S. Baek, and Y. Lim, "Origin-destination matrices estimated with a genetic algorithm from link traffic counts," *Transportation Research Record: Journal of the Transportation Research Board,* pp. 156-163, 2001.

[13] M. Florian and Y. Chen, "A Coordinate Descent Method for the Bi-level O–D Matrix Adjustment Problem," *International Transactions in Operational Research,* vol. 2, pp. 165-179, 1995.

[14] M. Li, T. Zhang, Y. Chen, and A. J. Smola, "Efficient mini-batch training for stochastic optimization," in *Proceedings of the 20th ACM SIGKDD international conference on Knowledge discovery and data mining*, 2014, pp. 661-670.

[15] M. Shafiei, M. Nazemi, and S. Seyedabrishami, "Estimating time-dependent origin–destination demand from traffic counts: extended gradient method," *Transportation Letters,* vol. 7, pp. 210-218, 2015.

[16] J. T. Lundgren and A. Peterson, "A heuristic for the bilevel origin–destination-matrix estimation problem," in *Transportation Research Part B: Methodological*, 2008, pp. 339-354.

[17] D. Masip, T. Djukic, M. Breen, and J. Casas, "Efficient OD Matrix Estimation Based on Metamodel for Nonlinear Assignment Function," presented at the Australasian Transport Research Forum 2018 Proceedings, Darwin, Australia, 2018.

[18] C. Antoniou, J. Barceló, M. Breen, M. Bullejos, J. Casas, E. Cipriani*, et al.*, "Towards a generic benchmarking platform for origin–destination flows estimation/updating algorithms: Design, demonstration and validation," *Transportation Research Part C: Emerging Technologies,* vol. 66, pp. 79-98, 2016.

[19] T. Djukic, S. Hoogendoorn, and H. Van Lint, "Reliability assessment of dynamic OD estimation methods based on structural similarity index," in *Transportation Research Board 92nd Annual Meeting*, 2013.

[20] M. Bierlaire and P. L. Toint, "Meuse: An origin-destination matrix estimator that exploits structure," *Transportation Research Part B: Methodological,* vol. 29, pp. 47-60, 1995.

[21] Y. J. Gur, "Estimation of an origin-destination trip table based on observed link volumes and turning movements. Executive summary," Federal Highway Administration, Washinton D.C.1980.

[22] H. Yang, "Heuristic algorithms for the bilevel origin-destination matrix estimation problem," in *Transportation Research Part B: Methodological*, 1995, pp. 231-242.

[23] G. Cantelmo, F. Viti, C. Tampêre, E. Cipriani, and M. Nigro, "Two-Step approach for correction of seed matrix in dynamic demand estimation," in *Transportation Research Record: Journal of the Transportation Research Board*, 2014, pp. 125-133.

[24] J. Doblas and F. G. Benitez, "An approach to estimating and updating origin–destination matrices based upon traffic counts preserving the prior structure of a survey matrix," *Transportation Research Part B: Methodological,* vol. 39, pp. 565-591, 2005.

[25] M. R. Nasab and Y. Shafahi, "Estimation of origin–destination matrices using link counts and partial path data," *Transportation,* pp. 1-28, 2019.

[26] C. Antoniou, M. Ben-Akiva, and H. N. Koutsopoulos, "Incorporating automated vehicle identification data into origin-destination estimation," in *Transportation Research Record*, 2004, pp. 37-44.

[27] C. Antoniou, M. Ben-Akiva, and H. N. Koutsopoulos, "Dynamic traffic demand prediction using conventional and emerging data sources," in *IEE Proceedings-Intelligent Transport Systems*, 2006, pp. 97-104.

[28] X. Yang, Y. Lu, and W. Hao, "Origin-destination estimation using probe vehicle trajectory and link counts," *Journal of Advanced Transportation,* vol. 2017, 2017.

[29] G. Michau, N. Pustelnik, P. Borgnat, P. Abry, A. Nantes, A. Bhaskar*, et al.*, "A primal-dual algorithm for link dependent origin destination matrix estimation," *IEEE Transactions on Signal and Information Processing over Networks,* vol. 3, pp. 104-113, 2017.

[30] M. S. Iqbal, C. F. Choudhury, P. Wang, and M. C. González, "Development of origin–destination matrices using mobile phone call data," *Transportation Research Part C: Emerging Technologies,* vol. 40, pp. 63-74, 2014.

[31] M. Strickert, F.-M. Schleif, and U. Seiffert, "Gradients of pearson correlation for analysis of biomedical data," in *Proceedings of the Argentine Symposium on Artificial Intelligence (ASAI 2007).(To appear.)*, 2007.

[32] Aimsun, "Aimsun Next 8.4 User's Manual," in *Aimsun Next 8.3*, ed. Aimsun, Barcelona, Spain., 2019.

[33] A. Bhaskar and E. Chung, "Fundamental understanding on the use of Bluetooth scanner as a complementary transport data," *Transportation Research Part C: Emerging Technologies,* vol. 37, pp. 42-72, 2013.

[34] A. Bhaskar, M. Qu, A. Nantes, M. Miska, and E. Chung, "Is bus overrepresented in Bluetooth MAC scanner data? Is MAC-ID really unique?," *International Journal of Intelligent Transportation Systems Research,* vol. 13, pp. 119-130, 2015.

[35] G. Michau, A. Nantes, A. Bhaskar, E. Chung, P. Abry, and P. Borgnat, "Bluetooth data in an urban context: Retrieving vehicle trajectories," *IEEE Transactions on Intelligent Transportation Systems,* vol. 18, pp. 2377-2386, 2017.

[36] M. V. Chitturi, J. W. Shaw, J. R. Campbell IV, and D. A. Noyce, "Validation of Origin–Destination Data from Bluetooth Reidentification and Aerial Observation," *Transportation Research Record,* vol. 2430, pp. 116-123, 2014.

[37] OpenStreetMap, "An Introduction to OpenStreetMap," ed, 2014.

[38] ASGS. (2017). *Australian Statistical Geography Standard (ASGS)*. Available: http://www.abs.gov.au/websitedbs/D3310114.nsf/home/Australian+Statistical+Geography+Standard+(ASGS)

[39] C. Osorio, "High-dimensional offline OD calibration for stochastic traffic simulators of large-scale urban networks," in *Technical Report*, ed: Massachusetts Institute of Technology, 2017.

[40] K. N. Behara, A. Bhaskar, and E. Chung, "Classification of typical Bluetooth OD matrices based on structural similarity of travel patterns-Case study on Brisbane city," in *Transportation Research Board 97th Annual Meeting*, Washington DC, United States, 2018.

Krishna N.S. Behara submitted his PhD thesis to Queensland University of Technology, Brisbane, Australia and currently working as a Research Assistant in the same university. He holds a Master's degree in Transportation Engineering and Bachelor of Engineering (Honors) in Civil Engineering, both from Birla Institute of Technology and Science, Pilani, India. His research interests include transport data analytics and traffic modelling and simulation.

Dr Ashish Bhaskar is an Associate Professor at QUT. He holds a PhD degree from the Swiss Federal Institute of Technology, Lausanne (EPFL); Masters' degree from The University of Tokyo, Tokyo, Japan; and Bachelors' in Civil Engineering from the Indian Institute of Technology, Kanpur, India. His research interests includes transport data analytics, transport modelling and simulation, and traffic management and control.

Prof Edward Chung is a Professor at Hong Kong Polytechnic University and Adjunct Professor in Queensland University of Technology. He holds a Bachelor of Engineering with Honors and PhD from Monash University, Australia. His research interests include traffic management, machine learning and transport modelling.